Organic Electronics 34 (2016) 237–245

Contents lists available at ScienceDirect

Organic Electronics

journal homepage: www.elsevier.com/locate/orgel

Indolo[3,2,1-*jk*]carbazole based planarized CBP derivatives as host materials for PhOLEDs with low efficiency roll-off

Paul Kautny [a, 1], Zhongbin Wu [b, 1], Johanna Eichelter [a], Ernst Horkel [a], Berthold Stöger [c], Jiangshan Chen [b, **], Dongge Ma [b], Johannes Fröhlich [a], Daniel Lumpi [a, *]

[a] Institute of Applied Synthetic Chemistry, Vienna University of Technology, Getreidemarkt 9/163, A-1060 Vienna, Austria
[b] State Key Laboratory of Polymer Physics and Chemistry, Changchun Institute of Applied Chemistry, Chinese Academy of Sciences, Changchun 130022, China
[c] Institute of Chemical Technologies and Analytics, Vienna University of Technology, Getreidemarkt 9/164, A-1060 Vienna, Austria

ARTICLE INFO

Article history:
Received 11 January 2016
Received in revised form
18 April 2016
Accepted 21 April 2016
Available online 29 April 2016

Keywords:
Blue PhOLED
High triplet energy
Low efficiency roll-off
Planarized CPB derivatives
Structure property relationship

ABSTRACT

Three novel planarized CPB derivatives (**ICzCz**, **ICzPCz**, **ICzICz**) have been synthesized and characterized concerning applications as host materials for PhOLEDs. The incorporation of fully planar indolo[3,2,1-*jk*]carbazole (ICz) in the CBP scaffold has been systematically investigated, revealing a significant impact on molecular properties, such as improved thermal stability (t_g > 110 °C), high triplet energies (E_T > 2.81 eV) and charge transport properties. Employing the newly developed materials as host materials, efficient green PhOLEDs (CE_{max}: 60.1 cd A^{-1}, PE_{max}: 42.1 lm W^{-1}, EQE_{max}: 15.9%) with a remarkably low efficiency roll-off of 5% at 1000 cd m^{-2} as well as blue PhOLEDs (**ICzCz**) with a high PE of 26.1 lm W^{-1} have been realized. Hence, the first comprehensive report on the application of ICz as integral building block for electroluminescent materials is presented, establishing this particular structural motive as versatile structural motive in this field.

1. Introduction

Starting with the groundbreaking work of Forrest et al., in 1998 [1,2], great efforts have been made in the development of phosphorescent organic light emitting diodes (PhOLEDs), due to their high internal quantum efficiency [3–8]. In contrast to fluorescent OLEDs, phosphorescent transition metal emitters harvest singlet and triplet excitons simultaneously. Therefore, PhOLEDs can theoretically achieve 100% internal quantum efficiency [9,10].

To avoid triplet-triplet annihilation at high current rates and consequently high concentrations of long living triplet excitons, phosphorescent emitters have to be widely dispersed in an organic host material [11,12]. Carbazole derivatives are among the most frequently employed host materials due to high triplet energies (E_T) and good charge transport properties [7]. Among those 4,4′-bis(9-carbazolyl)biphenyl (CBP - Scheme 1) has been widely utilized as host material for various dopants in PhOLEDs [7,13]. However, CBP exhibits some major drawbacks, such as a low glass transition temperature (t_g: 62 °C) [14] and a low E_T (2.56 eV) [15] resulting in devices with inferior thermal stability [16] and inefficient energy transfer to high energy blue guest emitters [15,17]. Since the emission of blue light is inevitable for the application of PhOLEDs as lighting source many modifications have been suggested to overcome the intrinsic drawbacks of CBP. The main strategies focus on the interruption of the conjugated π–system in order to retain high E_Ts and can be divided into three categories: (i) incorporation of a saturated carbon- or heteroatom-bridge [18–21]; (ii) sterically induced torsion [22–24] and (iii) shortening of the π–system [24–27].

Recently, our group introduced the application of fully planar indolo[3,2,1-*jk*]carbazole (ICz) as electron donating moiety in bipolar host materials [28,29]. Inspired by our initial findings we aimed to further incorporate the ICz building block into the CBP scaffold benefitting from the effects of systematic planarization of the triarylamine moiety. Hence, the study reveals a novel design strategy for unipolar opto-electronic materials yielding thermally stable CBP derivatives in combination with high E_T values. Particularly recent improvements in synthetic accessibility of the ICz

** Corresponding author.
* Corresponding author.
E-mail addresses: jschen@ciac.ac.cn (J. Chen), daniel.lumpi@tuwien.ac.at (D. Lumpi).
[1] Contributed equally to this work.

http://dx.doi.org/10.1016/j.orgel.2016.04.036
1566-1199/

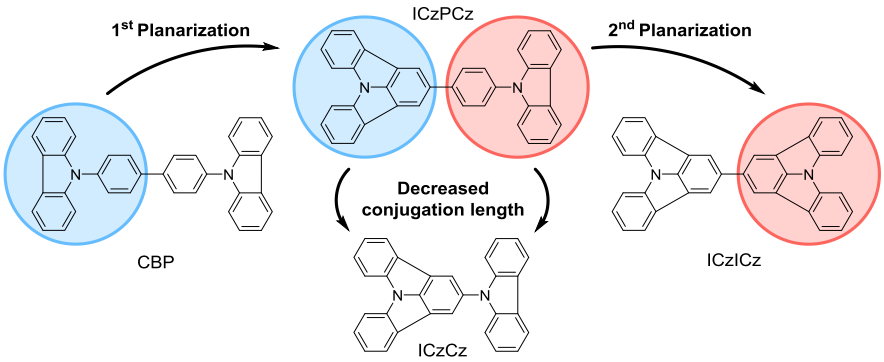

Scheme 1. Schematized molecular design of target materials **ICzCz**, **ICzPCz** and **ICzICz** by gradual planarization of the phenylcarbazole moieties.

moiety [28,30] elevate the relevance of revealing the application scope ICz based materials.

2. Materials and methods

2.1. General information

All reagents and solvents were purchased from commercial suppliers and used without further purification. Anhydrous solvents were prepared by filtration through drying columns. Column chromatography was performed on silica 60 (Merck, 40–63 μm). NMR spectra were recorded on a Bruker Avance DRX-400 Spectrometer. A Thermo Scientific LTQ Orbitrap XL hybrid FTMS (Fourier Transform Mass Spectrometer) equipped with a Thermo Fischer Exactive Plus Orbitrap (LC-ESI+) and a Shimadzu IT-TOF Mass Spectrometer were used for high resolution mass spectrometry. Thermogravimetric (TG) and differential scanning calorimetry (DSC) measurements were carried out with a heating rate of 5 K/min in a flowing argon atmosphere (25 ml/min). For the TG measurements, a Netzsch TG 209 F9 Tarsus system with open aluminium oxide crucibles was used. For the DSC measurements, a Netzsch DSC 200 F3 Maia, working with aluminium pans with pierced lids, was employed. UV/ViS absorption and fluorescence emission spectra were recorded in DCM solutions (5 μM) with a Perkin Elmer Lambda *750* spectrometer and an Edinburgh FLS920, respectively. Time resolved low temperature phosphorescence spectra were recorded in solid solutions (1 mg/ml; toluene:EtOH = 9:1) at 77 K with a Perkin Elmer Instruments LS 50B luminance spectrometer. Cyclic voltammetry was performed using a three electrode configuration consisting of a Pt working electrode, a Pt counter electrode and an Ag/AgCl reference electrode and a PGSTAT128N, ADC164, DAC164, External, DI048 potentiostat provided by Metrohm Autolab B.V. Measurements were carried out in a 0.5 mM solution in anhydrous DCM with Bu_4NBF_4 (0.1 M) as supporting electrolyte. The solutions were purged with nitrogen for 15 min prior to measurement. HOMO energy levels were calculated from the onset of the oxidation peaks. The onset potential was determined by the intersection of two tangents drawn at the background and the rising of the oxidation peaks.

2.2. Synthetic details

2-Bromoindolo[3,2,1-*jk*]carbazole (**1**) [31], 9-[4-(4,4,5,5-tetramethyl-1,3,2-dioxaborolan-2-yl)phenyl]-9*H*-carbazole (**3**) [32] and 2-(4,4,5,5-tetramethyl-1,3,2-dioxaborolan-2-yl)indolo[3,2,1-*jk*]-carbazole (**4**) [31] were synthesized according to previously published procedures whereas 9*H*-carbazole (**2**) was purchased by Apollo Scientific and used without further purification.

ICzCz. The synthesis of **ICzCz** was accomplished analogously to a published procedure [33]. **1** (3.20 g, 10.0 mmol, 1.00 eq.), **2** (2.50 g, 15.0 mmol, 1.50 eq.), K_2CO_3 (2.07 g, 15.0 mmol, 1.5 eq.) and $CuSO_4 \cdot 5H_2O$ (0.13 g, 0.5 mmol, 0.05 eq.) were ground and placed in a teflon autoclave, which was subsequently heated at 230 °C for 70 h. After cooling the solid was partitioned between CH_2Cl_2 and water and the aqueous phase was extracted with CH_2Cl_2. The combined organic layers were dried over anhydrous Na_2SO_4 and concentrated *in vacuo*. **ICzCz** (2.45 g, 6.0 mmol, 60%) was isolated after column chromatography (light petrol: CH_2Cl_2 = 80:20 → 50:50) as a yellowish white solid. ^{1}H NMR (400 MHz, CD_2Cl_2): δ = 8.24–8.20 (m, 4H), 8.16 (d, J = 7.7 Hz, 2H), 8.03 (d, J = 8.1 Hz, 2H), 7.65 (dd, J = 7.8, 7.8 Hz, 2H), 7.45–7.37 (m, 6H), 7.32 (ddd, J = 7.7, 6.6, 1.5 Hz, 2H) ppm. ^{13}C NMR (100 MHz, CD_2Cl_2): δ = 143.4 (s), 143.0 (s), 139.9 (s), 133.4 (s), 130.3 (s), 128.1 (d), 126.5 (d), 124.0 (d), 123.6 (s), 122.7 (d), 120.8 (d), 120.4 (d), 120.2 (d), 119.7 (s), 113.1 (d), 110.4 (d) ppm. Calculated: *m/z* 406.14645 $[M]^+$, 407.15428 $[M+H]^+$. Found: MS (ESI): *m/z* 406.14550 $[M]^+$, 407.15346 $[M+H]^+$.

ICzPCz. The Suzuki cross-coupling reaction towards ICzPCz was performed under an argon atmosphere. **1** (1.54 g, 4.80 mmol, 1.00 eq.) and boronic acid ester **3** (2.22 g, 6.00 mmol, 1.25 eq.) were dissolved in degassed THF (90 ml). Subsequently, 6 ml degassed aqueous K_2CO_3 (1.66 g, 12.00 mmol, 2.50 eq.) solution and $Pd(PPh_3)_4$ (0.28 g, 0.24 mmol, 0.05 eq.) were added and the reaction mixture was refluxed for 23 h (TLC). The solution was poured on water and repeatedly extracted with CH_2Cl_2. The combined organic layers were dried over anhydrous Na_2SO_4 and concentrated under reduced pressure. **ICzPCz** (1.38 g, 2.86 mmol, 60%) was isolated after column chromatography (light petrol: CH_2Cl_2 = 80:20 → 50:50) as a white solid. ^{1}H NMR (400 MHz, CD_2Cl_2): δ = 8.40 (s, 2H), 8.25 (d, J = 7.7 Hz, 2H), 8.19 (d, J = 7.7 Hz, 2H), 8.04 (d, J = 8.1 Hz, 2H), 7.98 (d, J = 8.1 Hz, 2H), 7.74 (d, J = 8.1 Hz, 2H), 7.63 (dd, J = 7.6, 7.7 Hz, 2H), 7.56 (d, J = 8.1 Hz, 2H), 7.49–7.41 (m, 4H), 7.33 (dd, 7.5, 7.3 Hz, 2H) ppm. ^{13}C NMR (100 MHz, CD_2Cl_2): δ = 144.3 (s), 143.0 (s), 141.5 (s), 139.8 (s), 137.2 (s), 136.8 (s), 130.5 (s), 130.1 (d), 127.9 (d), 127.7 (d), 126.6 (d), 123.9(2) (s), 123.8(6) (d), 122.5 (d), 120.8 (d), 120.5 (d), 119.8 (d), 119.3 (s), 113.0 (d), 110.4 (d) ppm. Calculated: *m/z* 482.17775 $[M]^+$, 483.18558 $[M+H]^+$. Found: MS (ESI): *m/z* 482.17699 $[M]^+$, 483.18510 $[M+H]^+$.

ICzICz. The Suzuki cross-coupling reaction towards **ICzICz** was performed under an argon atmosphere. **1** (1.54 g, 4.80 mmol, 1.00 eq.) and boronic acid ester **4** (2.20 g, 6.00 mmol, 1.25 eq.) were dissolved in degassed THF (90 ml). Subsequently, 6 ml degassed aqueous K_2CO_3 (1.66 g, 12.00 mmol, 2.50 eq.) solution and $Pd(PPh_3)_4$ (0.28 g, 0.24 mmol, 0.05 eq.) were added and the reaction mixture was refluxed 46 h (TLC). The precipitate was filtered and washed with THF and water. The filtrate and the aqueous phase

were combined resulting in further precipitation and filtered again. The solid was dissolved in CH_2Cl_2, the solution dried over anhydrous Na_2SO_4 and concentrated under reduced pressure yielding **ICzICz** (2.00 g, 4.16 mmol, 87%) as a white solid. ^{1}H NMR (400 MHz, CD_2Cl_2): δ = 8.46 (s, 4H), 8.25 (d, J = 7.6 Hz, 4H), 8.00 (d, J = 8.0 Hz, 4H), 7.63 (dd, J = 8.0, 7.6 Hz, 4H), 7.42 (dd, J = 7.6, 7.6 Hz, 4H) ppm. ^{13}C NMR (100 MHz, CD_2Cl_2): δ = 143.9 (s), 140.3 (s), 139.8 (s), 130.7 (s), 127.5 (d), 123.8 (d), 122.4 (d), 120.9 (d), 119.2 (s), 113.0 (d) ppm. Calculated: m/z 480.16210 $[M]^+$, 481.16993 $[M+H]^+$. Found: MS (ESI): m/z 480.16120 $[M]^+$, 481.16977 $[M+H]^+$.

2.3. Computational details

All (TD)DFT computations were performed using the Gaussian 09 package, revision D.01 [34]. Density functional theory (DFT) and time-dependent (TD)DFT calculations were performed using the Becke three parameters hybrid functional with Lee–Yang–Perdew correlation (B3LYP) [35,36], in combination with Pople basis sets (6–31G*, 6–311 + G*) [37]. Geometry optimizations were performed in gas phase and without symmetry constraints. For the calculation of HOMO/LUMO levels, ground state (S_0) geometries were optimized applying the 6–311 + G* basis set. The determination of triplet energy (E_T) was achieved by the calculation of the T_1 excitation energy applying TDDFT level and the 6–311 + G* basis to a S_0 geometry optimized at DFT level using the 6–31G* basis set. Orbital plots were generated using GaussView [38].

2.4. Single crystal diffraction

A crystal of **ICzCz** suitable for single crystal diffraction was selected under a polarizing microscope, embedded in perfluorinated oil and attached to Kapton® micromounts. Intensity data were collected in a dry stream of nitrogen at 100 K on a Bruker KAPPA APEX II diffractometer system. Data were reduced using SAINT-Plus [39] and an empirical absorption correction using the multi-scan approach implemented in SADABS [39] was applied. The crystal structures were solved by charge-flipping implemented in SUPERFLIP [40] and refined against F with the JANA2006 [41] software package. The non-H atoms were refined with anisotropic displacement parameters. The H atoms were placed at calculated positions and refined as riding on the parent C atoms.

2.5. Device fabrication and measurement

All the devices were fabricated on glass substrates pre-coated with 180 nm indium tin oxide (ITO) with a sheet resistance of 10 Ω per square. The ITO substrates were degreased in an ultrasonic solvent bath and then dried at 120 °C for 30 min. Before loaded into the deposition chamber, the ITO surface was treated with UV-ozone for 15 min. All layers were grown in succession by thermal evaporation without breaking the vacuum (<5 × 10^{-4} Pa). The device structures were described in the text. The organic materials and metal oxide were evaporated at the rate in a range of 1–2 Å/s, and the metals were evaporated at the rate of 8–10 Å/s. The overlap between ITO and Al electrodes was 4 mm × 4 mm which is the active emissive area of the devices. Current–voltage–brightness characteristics were measured by using a Keithley source measurement unit (Keithley 2400 and Keithley 2000) with a calibrated silicon photodiode. The EL spectra were measured on a Spectrascan PR650 spectrophotometer. EQEs were calculated from the luminance, current density, and EL spectrum, assuming a Lambertian distribution. All the measurements were carried out in ambient atmosphere.

3. Results and discussion

3.1. Molecular design

The aim of this work is to investigate the effects of a gradual planarization of the phenylcarbazole moieties of CBP on photophysical and electrochemical properties of the resulting materials. Starting from CBP, the planarization of one phenylcarbazole yields **ICzPCz** and the introduction of a second ICz group leads to twofold planarized **ICzICz**, which has been identified as dimeric product upon electrochemical oxidation of ICz [42] previously. Moreover, shortening the conjugated π-system of **ICzPCz** by removal of one phenyl unit results in **ICzCz**, which can be regarded as a planarized *para* derivative of *m*CP (Scheme 1).

3.2. Synthesis

The synthetic approach toward **ICzCz**, **ICzPCz** and **ICzICz** is outlined in Scheme 2. **ICzCz** was obtained in 60% yield *via* Ullmann condensation of bromoindolocarbazole **1** and carbazole **2** in the presence of $CuSO_4 \cdot 5H_2O$ and K_2CO_3. The synthesis of **ICzPCz** and **ICzICz** was accomplished in a Suzuki cross-coupling reaction employing **1** and the corresponding boronic acid esters **3** and **4**.

The chemical identity of the three title compounds was confirmed by ^{1}H and ^{13}C NMR measurements as well as high resolution mass spectroscopy. Additionally, single crystals of **ICzCz** [43] suitable for X-ray diffraction (Fig. 1) were grown from a CD_2Cl_2 solution by slow evaporation of the solvent at room temperature. The ICz moiety is virtually planar [maximum distance from the least squares (LS) planes: 0.043(2) Å for C29]. The carbazole and ICz moieties are distinctly inclined [angle between LS planes: 54.07(5) °].

3.3. Thermal properties

Thermal properties of the compounds were investigated by DSC and TGA (see supplementary material). All materials feature high thermal stability with decomposition temperatures (corresponding to 5% mass loss) higher than 344 °C. During DSC runs **ICzCz** and **ICzPCz** exhibited t_g values of 111 °C and 119 °C which are

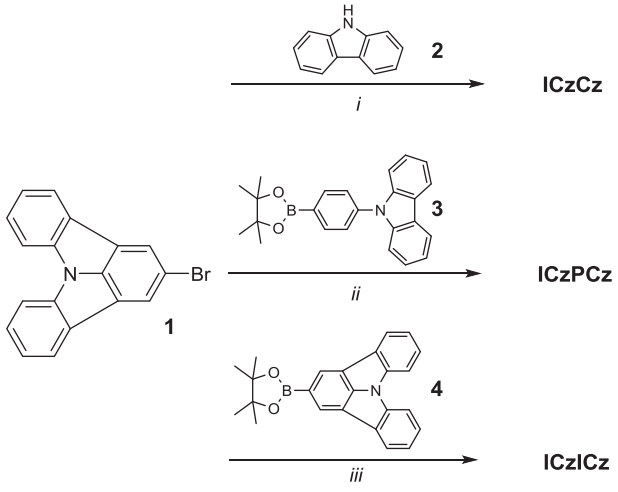

Scheme 2. Synthetic approach toward **ICzCz**, **ICzPCz** and **ICzICz**. *i*: **1** (1 eq.), **2** (1.5 eq.), K_2CO_3 (2.5 eq., 2 M aqueous solution), $CuSO_4 \cdot 5H_2O$ (0.05 eq.), 230 °C, 70 h, 60%; *ii*: **1** (1 eq.), **3** (1.25 eq.), $Pd(PPh_3)_4$ (0.05 eq.), K_2CO_3 (2.5 eq., 2 M aqueous solution), THF, reflux, 23 h, 60%; *iii*: **1** (1 eq.), **4** (1.25 eq.), $Pd(PPh_3)_4$ (0.05 eq.), K_2CO_3 (2.5 eq.), THF, reflux, 46 h, 87%.

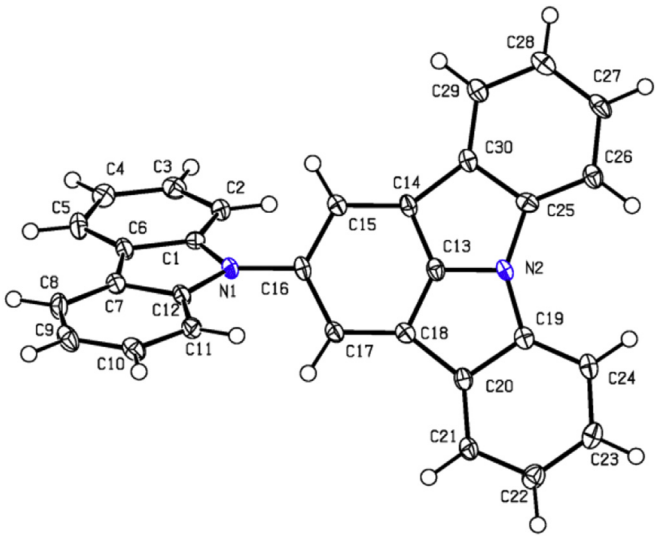

Fig. 1. Molecular structure of **ICzCz**; C and N atoms are represented by white and blue ellipsoids drawn at 50% probability levels, H atoms by spheres of arbitrary radius [44].

significantly higher compared to CBP (62 °C) [14]. The increased t_g values can be attributed to the high rigidity of the ICz motive. No t_g was observed in the case of **ICzICz** below the melting point 383 °C (decomposition).

3.4. Photophysical properties

To investigate the effects of the conducted molecular modifications on photophysical properties, UV/Vis absorption, photoluminescence as well as low temperature delayed photoluminescence were recorded. The spectra are displayed in Fig. 2. The compounds feature related absorption behavior with absorption onsets at 395 (**ICzCz**), 387 (**ICzPCz**) and 387 nm (**ICzICz**), corresponding to optical band gaps of 3.14, 3.21 and 3.21 eV, respectively. Compared to CBP (3.52 eV; see supplementary material) band gaps are reduced by more than 0.3 eV due to the lower band gap of the ICz building block in relation to phenylcarbazole [45], which benefits the fabrication of PhOLED devices with low driving voltage and high power efficiencies. All materials exhibit distinct absorption around 375 nm, which is attributed to the ICz motive. Furthermore, weak transitions at approximately 342 and 328 nm, typical values for phenylcarbazole derivatives [45], were observed for **ICzCz** and **ICzPCz**. Analogously, slightly blue-shifted absorption bands were found for **ICzICz** as shoulders at 332 and 316 nm. Prominent peaks below 300 nm are attributed to the $\pi-\pi^*$ transitions of the carbazole and/or ICz moieties [31,46]. Notably, in **ICzICz** the peak maximum at 292 nm is red-shifted compared to the other congeners; for **ICzCz** and **ICzPCz** this ICz derived transition is observed as shoulder in the absorption spectra. The corresponding carbazole related bands are located at lower wavelength.

ICzCz, **ICzPCz** and **ICzICz** exhibit photoluminescence with peak maxima at 404.5, 385.5 and 406 nm, respectively. Whereas **ICzCz** features unstructured emission, weak shoulders were observed at higher energies in the spectra of **ICzPCz** and **ICzICz**.

In order to gain insight into the photophysical properties of the potential host materials in the solid state, thin films were subjected to UV/Vis absorption and photoluminescence measurements (see supplementary material). Compared to measurements in solution absorption onsets are systematically red-shifted by approximately 10–20 nm due to intermolecular interactions. Emission spectra of

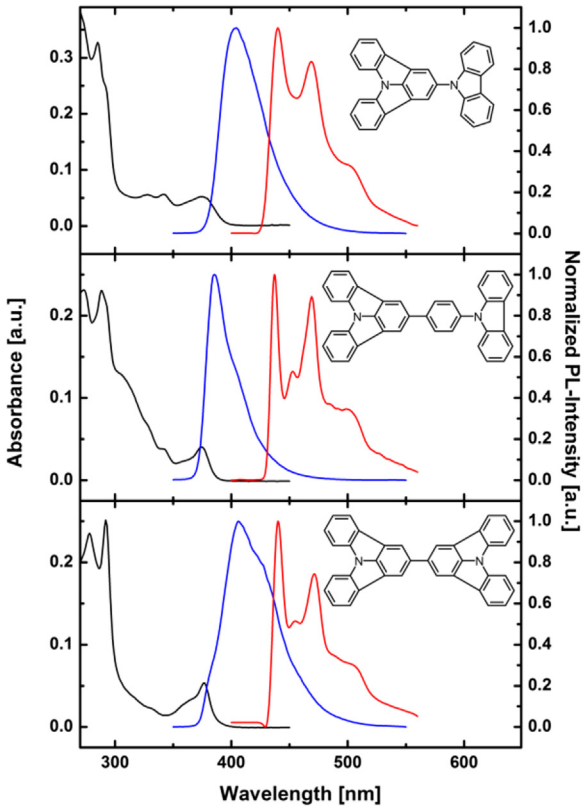

Fig. 2. UV–Vis absorption (black), normalized fluorescence spectra at room temperature (blue) and normalized phosphorescence spectra at 77 K (red) of **ICzCz** (top), **ICzPCz** (middle) and **ICzICz** (bottom). (For interpretation of the references to colour in this figure legend, the reader is referred to the web version of this article.)

thin films display a more diverse behavior. Whereas the emission of **ICzCz** is virtually identical in thin film and solution (peak maxima at 407 nm), thin film emission is slightly red-shifted in the case of **ICzPCz** (18.5 nm) and distinctly red-shifted for **ICzICz** (51 nm). Furthermore, additional low energy emission, indicating excimer formation upon photoexcitation, was observed around 550 nm, whereupon the intensity of this emission band increases from **ICzCz** to **ICzPCz** to **ICzICz**. These findings clearly indicate that the degree of excimer formation decreases in the order **ICzCz** < **ICzPCz** < **ICzICz**, which is in agreement with the tendency of planarized π-systems to aggregate in the solid state [47].

In contrast to room temperature fluorescence delayed phosphorescence spectra at 77 K exhibit well resolved vibronic peaks. Triplet energies calculated from the highest energy vibronic transition are 2.84, 2.82 and 2.82 eV for **ICzPCz**, **ICzCz** and **ICzICz**, respectively, which are significantly higher compared to CBP (2.56 eV) [15] and allow for the application of the developed ICz-hosts in blue PhOLED devices. Notably, the new host materials display a very low singlet-triplet energy splitting in the range of 0.28–0.39 eV. In fact, this is a particularly desirable feature, owing to a reduction of thermal losses during exciton transfer from the host to phosphorescent dopants retaining high power efficiency and enabling low driving voltage [8,48,49].

3.5. Electrical properties

The HOMO energy levels of the compounds were determined by cyclic voltammetric (CV) measurements (Fig. 3). All compounds exhibit irreversible oxidation, typically for carbazole and ICz materials [42,50]. HOMO levels were estimated from the onset of the

oxidation peak relative to ferrocene and are located at −5.56 eV for **ICzCz** and **ICzPCz**. However, in the case of **ICzICz** the HOMO is distinctly shifted to higher energy (−5.39 eV). A possible explanation for this unexpected electro-chemical behavior is given by DFT calculations (*vide infra*). LUMO levels were calculated from HOMOs and the optical bandgap determined from the UV/Vis absorption onset. The LUMO energy levels of **ICzCz** and **ICzPCz** are located at −2.42 and −2.35 eV, respectively, indicating no significant charge injection barriers from adjacent electron transporting layers. As a result of the increased HOMO level of **ICzICz** also the LUMO level is shifted to higher energy (−2.18 eV). The relevant photophysical and electrochemical data is summarized in Table 1.

3.6. Theoretical calculations

In order to provide a more detailed insight into the electronic properties of the developed materials at the molecular level, density functional theory (DFT) and time-dependent DFT (TDDFT) calculations were conducted using the Gaussian 09 software package [34]. Predicted HOMO and LUMO levels as well as E_T values are in good agreement with experimental data (Table 1). LUMO levels exhibit a systematic shift towards higher energies. Nevertheless, the tendency of increasing orbital energy from **ICzCz** to **ICzPCz** and **ICzICz** is reproduced by theoretical calculations.

The spatial distributions of HOMOs and LUMOs are significantly different in the investigated molecules (Fig. 4). Host materials **ICzCz** and **ICzPCz,** consisting of one indolocarbazole and carbazole moiety, feature distinctive separation of the HOMO and LUMO. Owing to the decreased donor strength of ICz [31], the LUMO is exclusively located on this particular molecular subunit in both compounds. Accordingly, the HOMO level spreads over the carbazole/phenylcarbazole and extends to some degree to the adjacent phenyl ring and nitrogen atom of the ICz. In this regard, although both subunits are arylamines, the carbazole acts as donor group, whereas ICz exhibits slight acceptor properties, a feature that has previously been observed in bipolar host materials by our groups [31]. In contrast the frontier molecular orbitals are uniformly distributed over the entire molecule in symmetric **ICzICz**. These findings are consistent with the electrochemical analysis of the materials and determine the energetic location of the orbitals. Whereas the HOMO of **ICzCz** and **ICzPCz** are located at −5.56 eV, typical for materials with electronically isolated carbazole groups [24,31,51,52], the HOMO level of **ICzICz** at −5.39 eV is increased due to a higher degree of delocalization.

Furthermore, the torsion angle between the planar subunits is a crucial parameter influencing intermolecular interaction in thin films [47]. Although geometry optimization of the molecules is carried out in the gas phase, the observed tendencies can be extrapolated to the solid state. Notably, the calculated torsion angle between the carbazole and ICz subunit in **ICzCz** is 73° and therefore significantly higher compared to the torsion angle between the indolocarbazoles in **ICzICz** (48°). This behavior can be attributed to the increased steric demand of the carbazole protons at C2 and C11 *meta* to the nitrogen atom (Fig. 1), which is not present in the case of ICz due to an altered annulation pattern. Analogously, the calculated torsion angle between the carbazole and the phenylene linker in **ICzPCz** is larger (61°) than between the phenylene linker and the ICz (42°). These results suggest an increased likelihood of intermolecular interaction of **ICzICz** molecules in the solid state compared to the other derivatives as consequence of a more planar overall molecular alignment [47], which is in line with enhanced excimer formation observed in **ICzICz** thin films (see supplementary material).

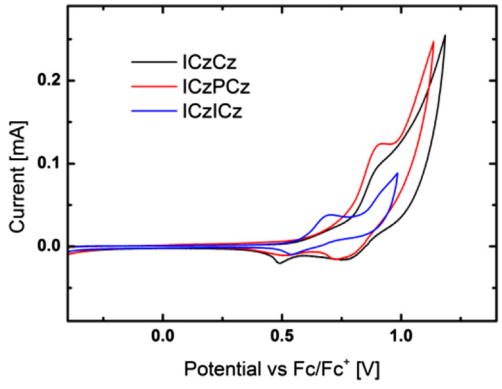

Fig. 3. CV curves of **ICzCz**, **ICzPCz** and **ICzICz**.

3.7. Electroluminescent properties

At first the applicability of the compounds as host materials in green PhOLEDs with the device architecture of ITO/MoO_3/TCTA: MoO_3 (20%, 50 nm)/TCTA (20 nm)/EML (20 nm)/BmPyPB (45 nm)/LiF/Al has been evaluated, whereby the EML was made up from 8 wt% green emitting Ir(ppy)$_2$(acac) doped into **ICzCz** (**GI**), **ICzPCz** (**GII**) or **ICzICz** (**GIII**). TCTA was used as a hole transporting layer and BmPyPB was employed as an electron transporting and hole blocking layer. Current density-voltage-luminance and current efficiency-luminance-power efficiency curves of device **GI-III** are displayed in Fig. 6 and key electroluminescent parameters are summarized in Table 2. Energy level diagrams of all devices are provided in the supplementary material. Exclusively green emission from Ir(ppy)$_2$(acac) was observed in all devices indication energy transfer from the host to the dopant (Fig. 5).

Devices **GI** and **GII** displayed similar performance, featuring high maximum current efficiencies (CE) of 60.1 cd A^{-1} and 56.3 cd A^{-1}, maximum power efficiencies (PE) of 36.5 lm W^{-1} and 35.4 lm W^{-1} and maximum external quantum efficiencies (EQE) of 15.9 and 14.8%, respectively. However, it has to be noted that CBP based PhOLEDs with the same devices architecture exhibited higher efficiency (CE_{max}: 84.7 cd A^{-1}; Supplementary Material). Nonetheless, **GI** and **GII** displayed satisfying characteristics and more notably both devices exhibited remarkably low efficiency roll-off. At a brightness of 1000 cd m^{-2}, relevant for practical applications, the CEs of **GI** and **GII** were still as high as 57.2 cd A^{-1} and 53.8 cd A^{-1}, corresponding to a negligible efficiency roll-off of 4–5%. Even at a high luminance of 5000 cd m^{-2} the devices reached CEs of 54.1 cd A^{-1} (**GI**; 10% roll-off) and 51.6 cd A^{-1} (**GII**; 8% roll-off). The observed efficiency roll-off is lower than for the corresponding CBP based device and can be explained by the partial bipolar character of **ICzCz** and **ICzPCz** as suggested by the theoretical calculations. In contrast, the electroluminescent performance of device **GIII** was distinctly lower and the **ICzICz** based PhOLED reached a CE_{max} of 32.9 cd A^{-1}, a PE_{max} of 23.0 lm W^{-1} and an EQE_{max} of 8.7%.

Subsequently, the ICz derivatives were probed as host materials for blue emitting FIrPic, according to the high E_Ts of the materials. However, blue emission from FIrPic could not be observed in devices employing **ICzPCz** and **ICzICz** as host materials for the phosphorescent dopant. Exclusively **ICzCz** based device **BI** with the architecture of ITO/MoO_3/TAPC (60 nm)/*m*CP (5 nm)/**ICzCz**: FIrPic (20 nm, 20%)/TmPyPB (30 nm)/LiF/Al displayed the expected emission as displayed in Fig. 7. TAPC was employed as hole transporting layer, owing to its higher hole mobility rate compared to TCTA [53] and mCP functions as exciton blocking layer because of its high E_T [25]. TmPyPB instead of BmPyPB was used as electron

Table 1
Physical data of target materials.

	$T_g/T_{rc}/T_m/T_d$ [°C][a]	Opt. BG [eV][b,c]	$\lambda_{PL,max}$ [nm][c]	HOMO/LUMO [eV]		E_T (eV)	
				exp.[d]	cal.[e]	exp.[f]	cal.[g]
ICzCz	111/156/253/344	3.14	404.5	−5.56/−2.42	−5.60/−1.91	2.82	2.87
ICzPCz	119/165/262/385	3.21	385.5	−5.56/−2.35	−5.60/−1.81	2.84	2.91
ICzICz	n.o.[h]/n.o.[h]/383[i]/408	3.21	406.0	−5.39/−2.18	−5.62/−1.71	2.82	2.91

[a] Determined from DSC/TGA analysis; T_{rc}: recrystallization temperature.
[b] Determined from the absorption onset.
[c] Measured in DCM (5 μM) at r.t.
[d] HOMO levels were calculated from the onset of the oxidation peak. CV-measurements were carried out in a 0.5 mM solution in anhydrous DCM with Bu_4NBF_4 (0.1 M) as supporting electrolyte; LUMO levels were calculated from HOMO levels and the optical bandgap.
[e] Calculated applying density functional theory level (B3LYP/6−311 + G*).
[f] Estimated from the highest energy vibronic transition in solid solutions of toluene/EtOH (9:1) at 77 K.
[g] Calculated applying the time-dependent density functional theory level (B3LYP/6−311 + G*).
[h] Not observed.
[i] Melts under decomposition.

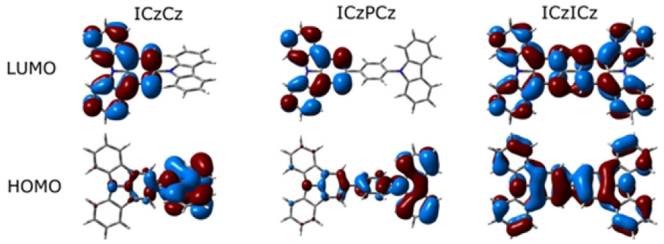

Fig. 4. Spatial distribution of HOMOs and LUMOs of the developed materials.

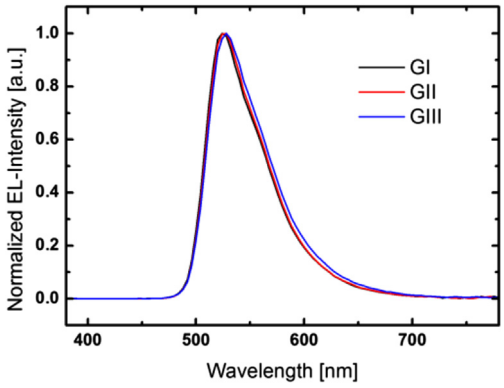

Fig. 5. Electroluminescence spectra of **GI**, **GII** and **GIII** at a driving voltage of 10 V.

transporting layer for **BI** due to its slightly higher E_T [6].

The surprising lack of FIrPic emission in devices with **ICzPCz** and **ICzICz** as host materials may be explained by the formation of excimers of the hosts in the emitting layer as result of the highly planar structure of the ICz moiety. Indeed red-shifted emission was observed in FIrPic doped **ICzICz** films (Figure S14). These excimers can act as triplet trapping sites, due to their low E_T and thus inhibit the confinement of triplet excitons on the phosphorescent emitter [54,55]. Notably, the tendency of **ICzPCz** and **ICzICz** to form excited dimers in the solid state is higher compared to **ICzCz** as suggested by thin film photoluminescence (see supplementary material). This fact is in line with the finding that FIrPic derived emission was exclusively observed in **BI** employing **ICzCz** as host materials. Among the three ICz derivatives **ICzICz** exhibits the highest tendency to aggregate in combination with red-shifted thin film emission (*vide supra*). Therefore, the high concentration of low triplet states in **ICzICz** thin films may not only impact blue devices but also impedes the energy transfer to green emitting Ir(ppy)$_2$(acac) in **GIII** and represents a possible explanation for the decreased efficiency of **GIII** compared to **GI** and **GII**. In contrast to FIrPic doped films the emission in **GIII** exclusively originates from the dopant. However, the energy of excimer emission of **ICzICz** is close to the emission of Ir(ppy)$_2$(acac). Thus, energy transfer from emissive excimer states to Ir(ppy)$_2$(acac) is reasonable. However, the presence of non-emissive low lying triplet states could significantly decrease the emission efficiency. Intermolecular interactions of carbazole derived host materials in thin films have recently been investigated and strongly depend on interchromophoric distances, a feature that can be efficiently addressed by subtle molecular modification [55]. This strategy can likewise be adapted to ICz based materials in order to minimize excimer formation.

Nevertheless, device **BI** showed a high performance with a CE_{max} of 32.8 cd A^{-1} and an EQE_{max} of 14.0%. Analogously to the green devices, **BI** exhibited low efficiency roll-off retaining a CE of 29.4 cd A^{-1} (10% roll-off) and 26.5 cd A^{-1} (19% roll-off) at 1000 cd m^{-2} and 5000 cd m^{-2}, respectively. Most notably device **BI** also featured a high PE_{max} of 26.1 lm W^{-1}. To the best of our knowledge, this value is among the highest compared to other biscarbazole derivatives connecting *via* the N atoms without an electron withdrawing subunit (Table 3). The high PE of **BI** is attributed to the small HOMO-LUMO gap and reduced singlet-triplet splitting of **ICzCz** compared to other CBP derivatives, thus allowing for efficient charge injection into the emitting layer and minimizing thermal energy losses upon exciton formation and energy transfer to FIrPic [8,48,49].

4. Conclusion

In this study the impact of incorporating fully planar indolo[3,2,1-*jk*]carbazole in the CBP scaffold has been systematically investigated. This strategy significantly improved the molecular properties of the target materials leading to: (i) better thermal stability owing to the rigid layout of the ICz motive; (ii) increased E_Ts and low singlet-triplet splitting enabling the application as host materials in blue PhOLEDs with high PE; (iii) low efficiency roll-off at high brightness, which is attributed to the chemical structure incorporating both the ICz and Cz moiety in one molecule. With these results the applicability of the ICz as universal building block for functional organic materials is being established. Further work will focus on controlling the intermolecular interactions of ICz based materials in the solid state by molecular design for the development of highly efficient ICz based materials for electroluminescent devices.

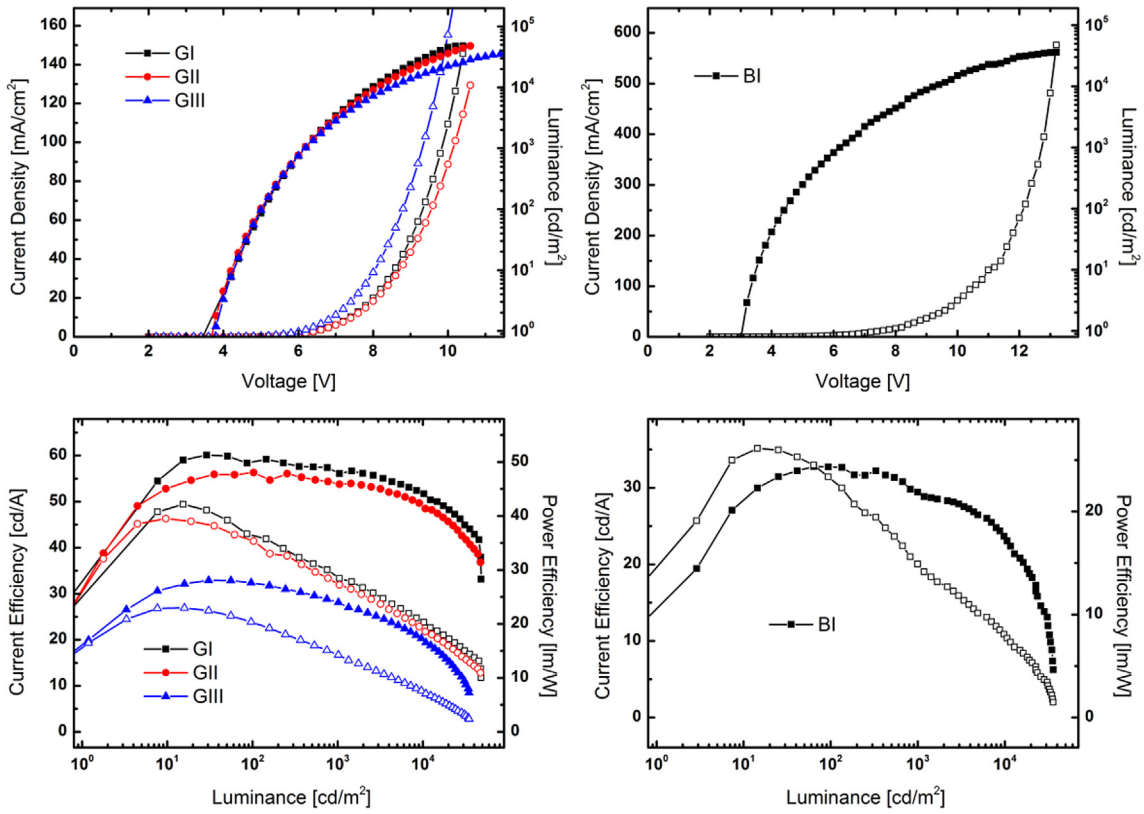

Fig. 6. Current density–voltage–luminance (hollow symbols: current density; full symbols: luminance) and current efficiency–luminance–power efficiency (full symbols: current efficiency; hollow symbols: power efficiency) curves of devices **GI-III** and **BI**.

Table 2
Electroluminescent properties of devices **GI-III** and **BI**.

	V_{on} [V]	CE [cd A^{-1}][a]	PE [lm W^{-1}][a]	EQE [%][a]
GI	3.8	58.5/57.2/54.1/60.1	36.5/28.5/23.5/42.1	15.6/14.9/14.2/15.9
GII	3.8	56.3/53.8/51.6/56.3	35.4/27.2/21.9/39.5	14.8/14.1/13.5/14.8
GIII	3.8	32.4/28.1/23.5/32.9	20.3/14.1/9.6/23.0	8.6/7.4/6.1/8.7
BI	3.2	32.7/29.4/26.5/32.8	23.4/14.9/10.1/26.1	14.0/12.7/11.4/14.0

[a] Measured at a brightness of 100 cd m^{-2}/1000 cd m^{-2}/5000 cd m^{-2}/max.

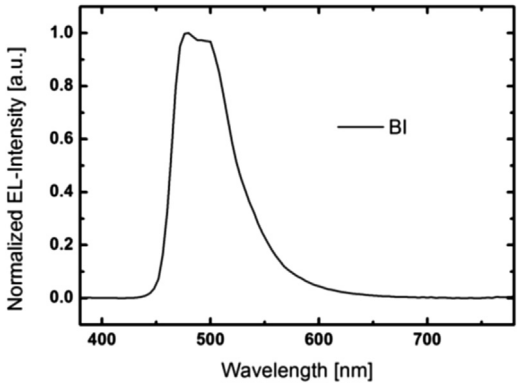

Fig. 7. Electroluminescence spectra of **BI** at a driving voltage of 10 V.

Table 3
Physical properties and device performance of FIrPic devices based on selected CBP derivatives.[a]

Host	T_g [°C]	E_T [eV]	PE [lm W^{-1}][b]	EQE [%][b]	Ref.
CBP	62 [14]	2.56	6.3	5.7	[15]
***m*CP**	60 [7]	2.90	9.3	12.3	[26]
CDBP	–	3.0	10.5	10.4	[22]
3CZPBP	110	–	17.3	16.5	[23]
***o*-CBP**	82	3.00	25.3	14.2	[24]
CBPE	81	3.01	5.1	–	[20]
DCz	–	2.95	15.0	9.8	[19]
CTP-3	113	2.81	25.6	15.4	[27]
DCB	–	2.95	–	5.8	[18]
ICzCz	111	2.82	26.1	14.0	This work

[a] Only CBP derivatives featuring two carbazole moieties connecting *via* the N atoms have been considered (see supplementary material).
[b] Maximum power efficiency and external quantum efficiency.

Acknowledgement

This work was supported in part by the Vienna University of Technology research funds and the Austrian Federal Ministry of Science, Research and Economy. The X-ray centre of the Vienna University of Technology is acknowledged for providing access to the single-crystal diffractometer.

Appendix A. Supplementary data

Supplementary data related to this article can be found at http://dx.doi.org/10.1016/j.orgel.2016.04.036.

References

[1] M.A. Baldo, D.F. O'Brien, Y. You, A. Shoustikov, S. Sibley, M.E. Thompson, S.R. Forrest, Highly efficient phosphorescent emission from organic electroluminescent devices, Nature 395 (1998) 151–154.

[2] M.A. Baldo, S. Lamansky, P.E. Burrows, M.E. Thompson, S.R. Forrest, Very high-efficiency green organic light-emitting devices based on electrophosphorescence, Appl. Phys. Lett. 75 (1999) 4–6.

[3] S.R. Forrest, The path to ubiquitous and low-cost organic electronic appliances on plastic, Nature 428 (2004) 911–918.

[4] Y. Sun, N.C. Giebink, H. Kanno, B. Ma, M.E. Thompson, S.R. Forrest, Management of singlet and triplet excitons for efficient white organic light-emitting devices, Nature 440 (2006) 908–912.

[5] S. Reineke, F. Lindner, G. Schwartz, N. Seidler, K. Walzer, B. Lussem, K. Leo, White organic light-emitting diodes with fluorescent tube efficiency, Nature 459 (2009) 234–238.

[6] L. Xiao, Z. Chen, B. Qu, J. Luo, S. Kong, Q. Gong, J. Kido, Recent progresses on materials for electrophosphorescent organic light-emitting devices, Adv. Mater 23 (2011) 926–952.

[7] Y. Tao, C. Yang, J. Qin, Organic host materials for phosphorescent organic light-emitting diodes, Chem. Soc. Rev. 40 (2011) 2943–2970.

[8] S. Reineke, M. Thomschke, B. Lüssem, K. Leo, White organic light-emitting diodes: Status and perspective, Rev. Mod. Phys. 85 (2013) 1245–1293.

[9] M.A. Baldo, D.F. O'Brien, M.E. Thompson, S.R. Forrest, Excitonic singlet-triplet ratio in a semiconducting organic thin film, Phys. Rev. B 60 (1999) 14422–14428.

[10] C. Adachi, M.A. Baldo, M.E. Thompson, S.R. Forrest, Nearly 100% internal phosphorescence efficiency in an organic light-emitting device, J. Appl. Phys. 90 (2001) 5048–5051.

[11] M.A. Baldo, C. Adachi, S.R. Forrest, Transient analysis of organic electrophosphorescence. II.Transient analysis of triplet-triplet annihilation, Phys. Rev. B 62 (2000) 10967–10977.

[12] C. Murawski, K. Leo, M.C. Gather, Efficiency roll-off in organic light-emitting diodes, Adv. Mater 25 (2013) 6801–6827.

[13] D.F. O'Brien, M.A. Baldo, M.E. Thompson, S.R. Forrest, Improved energy transfer in electrophosphorescent devices, Appl. Phys. Lett. 74 (1999) 442–444.

[14] M.H. Tsai, Y.H. Hong, C.H. Chang, H.C. Su, C.C. Wu, A. Matoliukstyte, J. Simokaitiene, S. Grigalevicius, J.V. Grazulevicius, C.P. Hsu, 3-(9-carbazolyl) carbazoles and 3,6-di(9-carbazolyl)carbazoles as effective host materials for efficient blue organic electrophosphorescence, Adv. Mater 19 (2007) 862–866.

[15] C. Adachi, R.C. Kwong, P. Djurovich, V. Adamovich, M.A. Baldo, M.E. Thompson, S.R. Forrest, Endothermic energy transfer: a mechanism for generating very efficient high-energy phosphorescent emission in organic materials, Appl. Phys. Lett. 79 (2001) 2082–2084.

[16] Y. Shirota, Organic materials for electronic and optoelectronic devices, J. Mater. Chem. 10 (2000) 1–25.

[17] I. Tanaka, Y. Tabata, S. Tokito, Energy-transfer and light-emission mechanism of blue phosphorescent molecules in guest-host systems, Chem. Phys. Lett. 400 (2004) 86–89.

[18] G.T. Lei, L.D. Wang, L. Duan, J.H. Wang, Y. Qiu, Highly efficient blue electrophosphorescent devices with a novel host material, Synth. Met. 144 (2004) 249–252.

[19] D.R. Whang, Y. You, S.H. Kim, W.I. Jeong, Y.S. Park, J.J. Kim, S.Y. Park, A highly efficient wide-band-gap host material for blue electrophosphorescent light-emitting devices, Appl. Phys. Lett. 91 (2007).

[20] J. He, H. Liu, Y. Dai, X. Ou, J. Wang, S. Tao, X. Zhang, P. Wang, D. Ma, Nonconjugated carbazoles: a series of novel host materials for highly efficient blue electrophosphorescent OLEDs, J. Phys. Chem. C 113 (2009) 6761–6767.

[21] D.H. Hu, P. Lu, C.L. Wang, H. Liu, H. Wang, Z.M. Wang, T. Fei, X. Gu, Y.G. Ma, Silane coupling di-carbazoles with high triplet energy as host materials for highly efficient blue phosphorescent devices, J. Mater. Chem. 19 (2009) 6143–6148.

[22] S. Tokito, T. Iijima, Y. Suzuri, H. Kita, T. Tsuzuki, F. Sato, Confinement of triplet energy on phosphorescent molecules for highly-efficient organic blue-light-emitting devices, Appl. Phys. Lett. 83 (2003) 569–571.

[23] Y. Agata, H. Shimizu, J. Kido, Syntheses and properties of novel quarterphenylene-based materials for blue organic light-emitting devices, Chem. Lett. 36 (2007) 316–317.

[24] S.L. Gong, X. He, Y.H. Chen, Z.Q. Jiang, C. Zhong, D.G. Ma, J.G. Qin, C.L. Yang, Simple CBP isomers with high triplet energies for highly efficient blue electrophosphorescence, J. Mater. Chem. 22 (2012) 2894–2899.

[25] R.J. Holmes, S.R. Forrest, Y.-J. Tung, R.C. Kwong, J.J. Brown, S. Garon, M.E. Thompson, Blue organic electrophosphorescence using exothermic host–guest energy transfer, Appl. Phys. Lett. 82 (2003) 2422–2424.

[26] S.J. Yeh, M.F. Wu, C.T. Chen, Y.H. Song, Y. Chi, M.H. Ho, S.F. Hsu, C.H. Chen, New dopant and host materials for blue-light-emitting phosphorescent organic electroluminescent devices, Adv. Mater 17 (2005) 285–289.

[27] L.S. Cui, S.C. Dong, Y. Liu, Q. Li, Z.Q. Jiang, L.S. Liao, A simple systematic design of phenylcarbazole derivatives for host materials to high-efficiency phosphorescent organic light-emitting diodes, J. Mater Chem. C 1 (2013) 3967–3975.

[28] P. Kautny, D. Lumpi, Y. Wang, A. Tissot, J. Bintinger, E. Horkel, B. Stöger, C. Hametner, H. Hagemann, D. Ma, J. Fröhlich, Oxadiazole based bipolar host materials employing planarized triarylamine donors for RGB PHOLEDs with low efficiency roll-off, J. Mater. Chem. C 2 (2014) 2069–2081.

[29] H. Puntscher, P. Kautny, B. Stoeger, A. Tissot, C. Hametner, H.R. Hagemann, J. Froehlich, T. Baumgartner, D. Lumpi, Structure-property studies of P-triarylamine-substituted dithieno[3,2-b:2',3'-d]phospholes, RSC Adv. 5 (2015) 93797–93807.

[30] J. Lv, Q. Liu, J. Tang, F. Perdih, K. Kranjc, A facile synthesis of indolo[3,2,1-jk] carbazoles via palladium-catalyzed intramolecular cyclization, Tetrahedron Lett. 53 (2012) 5248–5252.

[31] P. Kautny, D. Lumpi, Y. Wang, A. Tissot, J. Bintinger, E. Horkel, B. Stöger, C. Hametner, H. Hagemann, D. Ma, J. Fröhlich, Oxadiazole based bipolar host materials employing planarized triarylamine donors for RGB PHOLEDs with low efficiency roll-off, J. Mater Chem. C 2 (2014) 2069–2081.

[32] R. Anémian, D.C. Cupertino, P.R. Mackie, S.G. Yeates, Solution phase studies towards the synthesis of triarylamine oligomers using a germanium linker on a solid support, Tetrahedron Lett. 46 (2005) 6717–6721.

[33] H. Xu, K. Yin, W. Huang, Highly improved electroluminescence from a series of novel EuIII complexes with functional single-coordinate phosphine oxide ligands: tuning the intramolecular energy transfer, morphology, and carrier injection ability of the complexes, Chem. A Eur. J. 13 (2007) 10281–10293.

[34] M.J. Frisch, G.W. Trucks, H.B. Schlegel, G.E. Scuseria, M.A. Robb, J.R. Cheeseman, G. Scalmani, V. Barone, B. Mennucci, G.A. Petersson, H. Nakatsuji, M. Caricato, X. Li, H.P. Hratchian, A.F. Izmaylov, J. Bloino, G. Zheng, J.L. Sonnenberg, M. Hada, M. Ehara, K. Toyota, R. Fukuda, J. Hasegawa, M. Ishida, T. Nakajima, Y. Honda, O. Kitao, H. Nakai, T. Vreven, J.A. Montgomery Jr., J.E. Peralta, F. Ogliaro, M. Bearpark, J.J. Heyd, E. Brothers, K.N. Kudin, V.N. Staroverov, R. Kobayashi, J. Normand, K. Raghavachari, A. Rendell, J.C. Burant, S.S. Iyengar, J. Tomasi, M. Cossi, N. Rega, N.J. Millam, M. Klene, J.E. Knox, J.B. Cross, V. Bakken, C. Adamo, J. Jaramillo, R. Gomperts, R.E. Stratmann, O. Yazyev, A.J. Austin, R. Cammi, C. Pomelli, J.W. Ochterski, R.L. Martin, K. Morokuma, V.G. Zakrzewski, G.A. Voth, P. Salvador, J.J. Dannenberg, S. Dapprich, A.D. Daniels, Oe Farkas, J.B. Foresman, J.V. Ortiz, J. Cioslowski, D.J. Fox, Gaussian 09, Revision D.01, Gaussian, Inc., Wallingford CT, 2009.

[35] C. Lee, W. Yang, R.G. Parr, Development of the Colle-Salvetti correlation-energy formula into a functional of the electron density, Phys. Rev. B 37 (1988) 785–789.

[36] A.D. Becke, Density-functional thermochemistry. III. The role of exact exchange, J. Chem. Phys. 98 (1993) 5648–5652.

[37] R. Krishnan, J.S. Binkley, R. Seeger, J.A. Pople, Self-consistent molecular orbital methods. XX. A basis set for correlated wave functions, J. Chem. Phys. 72 (1980) 650–654.

[38] R. Dennington, T. Keith, J. Millam, GaussView, Version 5, Semichem Inc., Shawnee Mission KS, 2009.

[39] Bruker Computer Programs: APEX2, SAINT, SADABS, and SHELXTL, Bruker AXS Inc., Madison WI, 2013.

[40] L. Palatinus, G. Chapuis, SUPERFLIP – a computer program for the solution of crystal structures by charge flipping in arbitrary dimensions, J. Appl. Crystallogr. 40 (2007) 786–790.

[41] V. Petříček, M. Dušek, L. Palatinus, Jana2006. The Crystallographic Computing System, Institute of Physics, Praha, Czech Republic, 2006.

[42] S.I. Wharton, J.B. Henry, H. McNab, A.R. Mount, The production and characterisation of novel conducting redox-active oligomeric thin films from electrooxidised Indolo[3,2,1-jk]carbazole, Chem. Eur. J. 15 (2009) 5482–5490.

[43] ICzCz: C30H18N2, Mr = 406.5, orthorhombic, Pca21, a = 18.372(8) Å, b = 4.0466(17) Å, c = 25.957(11) Å, V = 1929.8(14) Å3, Z = 4, μ = 0.082 mm-1, T = 100 K, 23 375 measured, 5594 independent and 4603 observed [I > 3σ(I)] reflections, 289 parameters, wR (all data) = 0.0767, R [I > 3σ(I)] = 0.0624; CCDC reference number 1442064.

[44] A.L. Spek, Structure validation in chemical crystallography, Acta Crystallogr. D. 65 (2009) 148–155.

[45] H.H. Li, Y. Wang, K. Yuan, Y. Tao, R.F. Chen, C. Zheng, X.H. Zhou, J.F. Li, W. Huang, Efficient synthesis of pi-extended phenazasilines for optical and electronic applications, Chem. Commun. 50 (2014) 15760–15763.

[46] Z. Ge, T. Hayakawa, S. Ando, M. Ueda, T. Akiike, H. Miyamoto, T. Kajita, M.-a. Kakimoto, Novel bipolar bathophenanthroline containing hosts for highly efficient phosphorescent OLEDs, Org. Lett. 10 (2008) 421–424.

[47] M. Mas-Torrent, C. Rovira, Role of molecular order and solid-state structure in organic field-effect transistors, Chem. Rev. 111 (2011) 4833–4856.

[48] D. Zhang, L. Duan, D. Zhang, J. Qiao, G. Dong, L. Wang, Y. Qiu, Extremely low driving voltage electrophosphorescent green organic light-emitting diodes based on a host material with small singlet-triplet exchange energy without p- or n-doping layer, Org. Electron. 14 (2013) 260–266.

[49] D. Zhang, L. Duan, Y. Li, H. Li, Z. Bin, D. Zhang, J. Qiao, G. Dong, L. Wang, Y. Qiu, Towards high efficiency and low roll-off orange electrophosphorescent devices by fine tuning singlet and triplet energies of bipolar hosts based on Indolocarbazole/1, 3, 5-Triazine hybrids, Adv. Funct. Mater. 24 (2014) 3551–3561.

[50] E. Mondal, W.-Y. Hung, H.-C. Dai, K.-T. Wong, Fluorene-based asymmetric bipolar universal hosts for white organic light emitting devices, Adv. Funct. Mater 23 (2013) 3096–3105.

[51] P. Kautny, Z. Wu, B. Stöger, A. Tissot, E. Horkel, J. Chen, D. Ma, H. Hagemann, J. Fröhlich, D. Lumpi, Controlling singlet–triplet splitting in carbazole–oxadiazole based bipolar phosphorescent host materials, Org. Electron 17

(2015) 216–228.
[52] Y. Tao, Q. Wang, C. Yang, C. Zhong, K. Zhang, J. Qin, D. Ma, Tuning the opto-electronic properties of carbazole/oxadiazole hybrids through linkage modes: hosts for highly efficient green electrophosphorescence, Adv. Funct. Mater 20 (2010) 304–311.
[53] J. Lee, N. Chopra, S.-H. Eom, Y. Zheng, J. Xue, F. So, J. Shi, Effects of triplet energies and transporting properties of carrier transporting materials on blue phosphorescent organic light emitting devices, Appl. Phys. Lett. 93 (2008) 123306.
[54] S.T. Hoffmann, P. Schrogel, M. Rothmann, R.Q. Albuquerque, P. Strohriegl, A. Kohler, Triplet excimer emission in a series of 4,4'-Bis(N-carbazolyl)-2,2'-biphenyl derivatives, J. Phys. Chem. B 115 (2011) 414–421.
[55] K.L. Woon, Z.A. Hasan, B.K. Ong, A. Ariffin, R. Griniene, S. Grigalevicius, S.-A. Chen, Triplet states and energy back transfer of carbazole derivatives, Rsc Adv. 5 (2015) 59960–59969.